Structural behavior of uranium dioxide under pressure by LSDA+U calculations

H. Y. Geng,[1] Y. Chen,[1] Y. Kaneta,[1] and M. Kinoshita[2,3]
[1]*Department of Quantum Engineering and Systems Science, The University of Tokyo, Hongo 7-3-1, Tokyo 113-8656, Japan*
[2]*Nuclear Technology Research Laboratory, Central Research Institute of Electric Power Industry, Tokyo 201-8511, Japan*
[3]*Japan Atomic Energy Agency, Ibaraki 319-1195, Japan*

(Received 24 August 2006; revised manuscript received 17 December 2006; published 22 February 2007)

The structural behavior of UO_2 under high pressure up to 300 GPa has been studied by first-principles calculations with LSDA+U approximation. The results show that a pressure-induced structural transition to the cotunnite-type (orthorhombic *Pnma*) phase occurs at 38 GPa. It agrees well with the experimentally observed ~42 GPa. An isostructural transition following that is also predicted to take place from 80 to 130 GPa, which has not yet been observed in experiments. Further high compression beyond 226 GPa will result in a metallic and paramagnetic transition. It corresponds to a volume of 90 $Å^3$ per cell, in good agreement with a previous theoretical analysis in the reduction of volume required to delocalize $5f$ states.

DOI: 10.1103/PhysRevB.75.054111 PACS number(s): 61.50.Ah, 61.50.Ks, 71.15.Nc, 71.27.+a

I. INTRODUCTION

Uranium dioxide (UO_2) is widely used as fuel material in nuclear reactors. Its physical, chemical, and thermodynamic properties have been extensively studied since the 1940s by experimental and theoretical methods (especially during last decade) due to its important applications.[1–6] The shortage of energy around the world makes us ask for more contribution from nuclear power, where the burn-up efficiency of nuclear fuels is a bottleneck. In order to tackle this difficulty, understanding the detailed behavior of fuel materials under burning-up and irradiation is important. Recent use of fuel materials to high burn-up shows many microstructure formations, which are not possible to access by an empirical approach and atomic-scale theoretical analysis is highly desired.[7,8]

Previous theoretical studies of UO_2 mainly focused on defect effects arising from irradiation damage[6,9] and thermodynamic properties near ambient pressure[1,10,11] with semiempirical approaches. Electronic properties and large-scale intrinsic structural behavior under disturbance (say, compression, tension, and distortion of lattices) were rarely investigated despite its importance in most properties of UO_2. This partly is due to the lack of a reliable method to deal with this kind of complex materials. The development of density functional theory (DFT) changed the situation greatly and provides a quantum-mechanics-based theoretical approach to tackle this problem.[12–14]

However, to our knowledge only a few *ab initio* electronic structure studies have been published on UO_2, most of which were based on the conventional local density approximation (LDA) or generalized gradient approximation (GGA) of the exchange-correlation energy.[3,4,15–18] It is well recognized that strong Coulomb correlation among partly filled f electrons of uranium atoms makes these approximations fail. Usually a metallic ground state is predicted for UO_2 instead of the experimentally observed antiferromagnetic semiconductor.[19,20] The same problem exists for transition metal oxides and raises questions about the applicability of DFT approach to these materials. Fortunately, a method combining the spin-polarized local density approximation (LSDA) and on-site Coulomb repulsion among localized d or f electrons[13,14]—namely, the LSDA+U method—was proposed and has shown its capability to treat this problem.[21,22]

Usually, a Hubbard Hamiltonian with two empirical parameters is employed to describe the Coulomb interaction between $5f$ electrons localized on uranium sites in UO_2. Adding this Hamiltonian to the conventional LSDA (or GGS) energy functional, one arrives at a point where all orbitals except those included in the model Hamiltonian are treated within the framework of the LSDA (or GGS) while the localized $5f$ states are treated by the unrestricted Hartree-Fock (UHF) approximation[22]: namely,

$$E_{\mathrm{LSDA}+U} = E_{\mathrm{LSDA}}[\{\varepsilon_i\}] + \frac{(U-J)}{2}\sum_{l,j,\sigma}\rho_{lj}^{\sigma}\rho_{jl}^{\sigma}, \qquad (1)$$

where ρ_{lj}^{σ} is the density matrix of electrons occupying a partly filled electron shell ($5f$ in UO_2), σ refers to the spin direction, and $\{\varepsilon_i\}$ are the Kohn-Sham eigenvalues. A self-consistent solution of DFT with this energy functional gives the result that strong correlation effects associated with $5f$ states are going to affect all other states as well; in particular, although $2p$ states of oxygen are not influenced by Hubbard correlations directly, they are really linked to localized $5f$ states via hybridization terms. It is necessary to point out that the LSDA+U method is not a self-determined approach. The results depend on the model parameters U and J very much, which should be chosen carefully by comparing with experimental data. Fortunately, this can be done very well with just a small set of data and it preserves the predicability of the method mostly.[20–22]

There have been several works with the LSDA+U approximation on uranium dioxide published. All of them were near the equilibrium volume at ambient pressure for fluorite structure and focused mainly on electron energy loss spectra[21–23] and magnetic structure.[24] These calculations showed that the results of LSDA+U are in good agreement with experiments. However, no attempt was made to investigate the structural behavior of UO_2 under pressures with the LSDA+U method, which may be fundamental for understanding the behavior of nuclear fuel under irradiations. By

far the validity of the LSDA+U method beyond fluorite structure for UO_2 has not been confirmed yet. A recent hydrostatic compression experiment[25] makes it possible to check it by comparing with the measured equation of state. On the other hand, first-principles calculations without Hubbard correction to the GGA(S) approximation showed that it can give almost correct energy information for UO_2,[3,4,18] regardless of the fact that a wrong electronic band structure was predicted. Especially, by calculating the lattice parameter and bulk modulus of fluorite structure UO_2 with various approximations, Boettger and Ray argued that density gradient corrections, spin polarization, and spin-orbit coupling effects are equally important and suggested that when only structural properties are concerned LSDA+U is not necessary.[15] However, the predicted wrong ferromagnetic ground state weakened the creditability of their argument. Other calculations ignoring spin-orbit coupling also gave a reasonable lattice parameter and bulk modulus[3,4,18] and indicate that spin-orbit coupling is not so important for this case (though a large impact on magnetic property is expected). We will show in this paper that one should be careful when the GGA(S) is used because the coincidence of cohesive energies of UO_2 calculated by the GGS with LSDA+U approximations is valid only for the fluorite phase. An energy difference will appear if other structures are involved.

In this paper, we will study the structural stability of the fluorite phase (with $Fm\bar{3}m$ space group) and cotunnite phase (*Pnma* space group) of uranium dioxide under hydrostatic pressures using the DFT method based on the LSDA and GGS plus Hubbard correction. The calculation methodology is presented briefly in the next section. We will discuss a little bit about the widely used rule of common tangent of energy curves to determine the transition pressure of pressure-induced structural transitions, because this rule fails in the case when an energy barrier exists. A more general rule is proposed, which can give the energy barrier when the experimental transition pressure is available. Finally, a detailed comparison of our results with static high-pressure experiments is given, accompanied by a discussion on the ultrahigh-pressure behavior of UO_2 crystal.

II. METHODOLOGY

Total energy curves of both phases (*Pnma* and $Fm\bar{3}m$) at different volumes are computed with the VASP code.[26,27] The *Pnma* structure is fully relaxed to get all Hellman-Feynman forces smaller than 0.002 eV/Å, while fluorite structure keeps the ideal geometry due to all coordinates are completely determined by the symmetry. For comparison, both the spin-polarized generalized gradient approximation[28] (GGS) and local density approximation[29] (LSDA) with and without the Hubbard U term energy functional are used. The parameters of the Hubbard term are taken as $U=4.5$ eV and $J=0.51$ eV, which was checked carefully by Dudarev *et al.* for fluorite UO_2.[20–22] Calculations employed projector-augmented-wave (PAW) pseudopotentials[30,31] with a cutoff kinetic energy for plane waves of 400 eV. Integrations in reciprocal space are performed in the first Brillouin zone with 18 irreducible k points for fluorite structure and at least 28 irreducible k points for cotunnite phase generated with the Monkhorst-Pack[32] scheme. Its convergence is checked well. The energy tolerance for the charge self-consistency convergence is set to 1×10^{-5} eV for all calculations. Cohesive energies at different volumes are extracted from the total energies by subtracting spin-polarized isolated atom contributions. Then, they are fitted to a Morse-type energy function

$$E(V) = D[(e^{-g[(V/V_0)^{1/3}-1]/2} - 1)^2 - 1] \tag{2}$$

to facilitate post-analysis. It is necessary to point out that for the *Pnma* phase we also used a different U value obtained by fitting to experimental data of the *Pnma* phase since $U=4.5$ eV fails to predict the correct transition pressure. This implies that structure or lattice distortions would have considerable impact on the on-site Coulomb interaction. For the same structure, however, we find that the dependence of U on pressure is ignorable.

The equation of state (or compression curve) at 0 K is calculated directly by an infinitesimal variation of the cohesive energy with respect to volume given by $P=-\partial E/\partial V$. Usually the phase transition pressure is determined by the common tangent of their energy curves, which can be derived simply as follows. At the thermodynamic equilibrium state under finite pressure, the enthalpy must be minimized—i.e., $\delta H=0$. In the case two phases are in equilibrium, there is a variation of the enthalpy with respect to the concentration of each phase besides with respect to volumes. The latter gives $P_i=-\partial E_i/\partial V$ (where i is the phase label) and the former results in $P=-\Delta E/\Delta V=(E_2-E_1)/(V_1-V_2)$ with $\delta H=\delta x(\Delta E+P\Delta V)$, where δx is the concentration variation of, say, the first phase and ΔE (ΔV) is the energy (volume) difference between these two phases. The balance condition of pressure requires $P=P_i$ (for $i=1,2$): namely,

$$-\left.\frac{\partial E_i}{\partial V}\right|_{V=V_i} = \frac{E_2-E_1}{V_1-V_2}. \tag{3}$$

It is exactly the common tangent rule for the transition pressure of pressure-induced structural transitions. Evidently, $P\Delta V$ provides the least energy ΔE required to drive a transition from phase 1 to phase 2. The transition pressure equals P if no energy barrier exists, which is a common case for the usual metals and alloys. However, when an energy barrier with an amplitude of Δw is involved,[33–35] the work done by external pressure P' should be large enough to get over the barrier in addition to the energy difference ΔE. Then the variation of enthalpy with respect to phase concentration should be $\delta H=(\Delta E+\Delta w+P'\Delta V)\delta x\equiv 0$. Obviously the common tangent rule becomes invalid here. The hysteresis pressure is given by $\Delta P=P'-P$. Without knowledge about the energy barrier, one cannot determine the transition pressure P' by the energy curves themselves. However, in contrast, one can deduce the energy barrier amplitude with measured transition pressure P' by

$$\Delta w = -(\Delta E + P'\Delta V). \tag{4}$$

TABLE I. Cohesive energies of uranium dioxide at 0 GPa.

Phase	Approach	D (eV/atom)	g	r_0 (Å)	B_0 (GPa)
$Fm\bar{3}m$	LSDA	9.044	6.122	5.323	239.99
$Fm\bar{3}m$	GGS	7.956	6.195	5.432	203.53
$Fm\bar{3}m$	LSDA+U	8.194	6.198	5.444	208.32
$Fm\bar{3}m$	GGS+U	7.212	6.336	5.552	180.68
$Fm\bar{3}m$	Other calc.	7.41[a], 8.2[c]		5.37[a], 5.24[b], 5.4[c]	173[a], 252[b], 194[c]
$Fm\bar{3}m$	Expt.	7.44[d]		5.46[d], 5.473[e]	207[e], 208.9[f]
Pnma	LSDA+U(U=4.5 eV)	8.154	5.787	5.331	192.5
Pnma	LSDA+U(U=6.0 eV)	8.020	5.972	5.340	200.6

[a]LMTO+LSDA+U (Ref. 21).
[b]PW+LDA (Ref. 17).
[c]PW+GGA (Ref. 18).
[d]Taken from Ref. 21.
[e]See Ref. 25.
[f]See Ref. 36.

III. CALCULATIONS AND DISCUSSIONS

A. Cohesive energy

Calculated cohesive energies with different approximations for fluorite ($Fm\bar{3}m$) and cotunnite (*Pnma*) structures of uranium dioxide as well as the parameters fitted to Eq. (2) are listed in Table I, where the energy is per atom and the equilibrium cell volume is given by $V_0=r_0^3$. The cohesive energy for a cell of U_4O_8 is given by multiplying D by 12. For comparison purposes, other calculated and observed values[17,18,21,25,36] are also listed. It should be noticed that the *Pnma* phase has a smaller effective cubic lattice constant and bulk modulus than the fluorite phase at zero pressure, which implies it will become stable under compression.

Variation of cohesive energy of the $Fm\bar{3}m$ phase along the cubic lattice constant ($V^{1/3}$) is shown in Fig. 1. It is interesting to see that GGS and LSDA+U give quite similar energy curves, confirming previous calculations that GGS also can give reasonable energy information for the fluorite phase of UO_2 in spite of the fact that the corresponding electronic density of states (DOS) is wrong.[4,15,18,37] However, we should emphasize here that it is just a coincidence. Analogous to the case without Hubbard correction, LSDA+U overestimates the binding energy slightly and GGS+U underestimates it. On the other hand, the U term uplifts the binding energy wholly and results in this coincidence. We can also see from Table I that the PAW method outperforms ordinary pseudopotentials both for GGS and LSDA approximations in terms of equilibrium volume, cohesive energy, and bulk modulus.[4,17,18] Furthermore, our LSDA+U calculations with PAW potentials give results in perfect agreement with experiments[21,25,36] (in particular, the calculated equilibrium lattice constant of 5.44 Å versus observed 5.46 Å and bulk modulus of 208.3 GPa vs 208.9 GPa). It also predicts an antiferromagnetic ground state with a band gap of ~1.45 eV and agrees with previous calculations very well.[21] To reproduce the x-ray photoelectron spectroscopy[38] observed band gap of ~2 eV, Dudarev *et al.* argued that to take spin-orbit coupling into account[22] is necessary. We confirmed this by a spin-orbit coupling calculation implemented in VASP which gives a band gap of 2.04 eV. The GGS+U approximation, however, gives a larger equilibrium lattice constant and smaller bulk modulus, despite the cohesive energy being closer to the observed value, as well as a band gap of 1.6 eV. Totally speaking, the LSDA+U outperforms GGS+U approximation for this set of U term parameters. It is necessary to point out that the discrepancy with a previous linear muffin-tin orbital (LMTO) calculation[21] owing to their convergence precision is not so good. Their calculation gave quite poor mechanical properties,[39] implying that the force is inaccurate. A later calculation by the same authors improved this.[22] The spin-orbit coupling is ignored in our following calculations. The resulting error can be estimated at a lattice constant of 5.44 Å for the fluorite phase, where spin-orbit

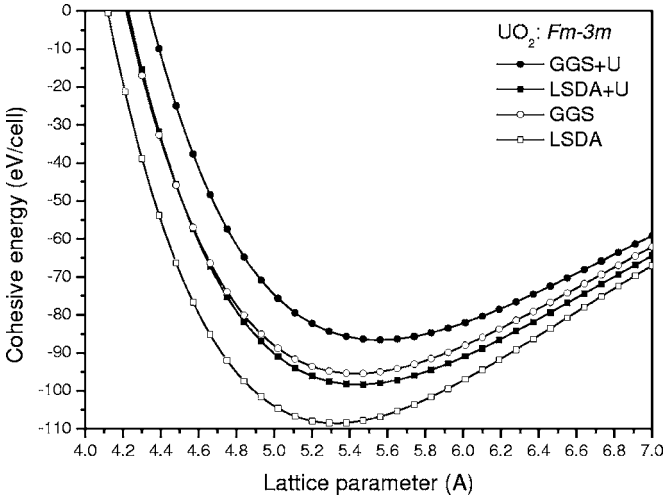

FIG. 1. Comparison of cohesive energy curves for fluorite structure of UO_2 calculated by LSDA, GGS, LSDA+U, and GGS+U approximations, respectively. Notice GGS and LSDA+U approximations give very close energy, especially at the high-compression region.

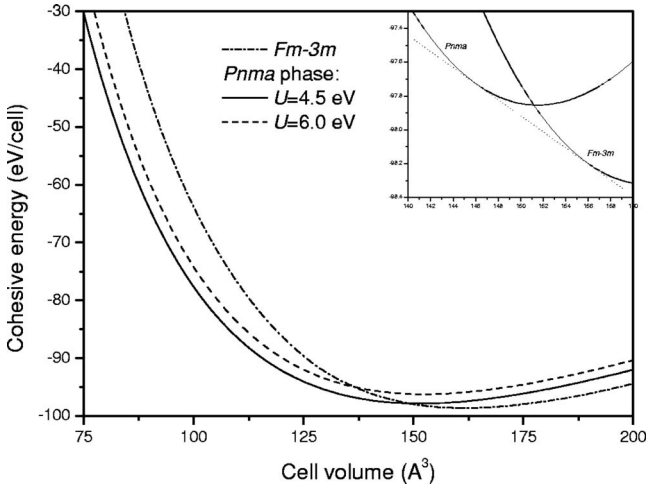

FIG. 2. Comparison of cohesive energies of *Pnma* and $Fm\bar{3}m$ phases along the cell volume. A phase transition at 7.8 GPa is predicted by the slope of the common tangent rule for the $U=4.5$ eV case, as shown in the inset.

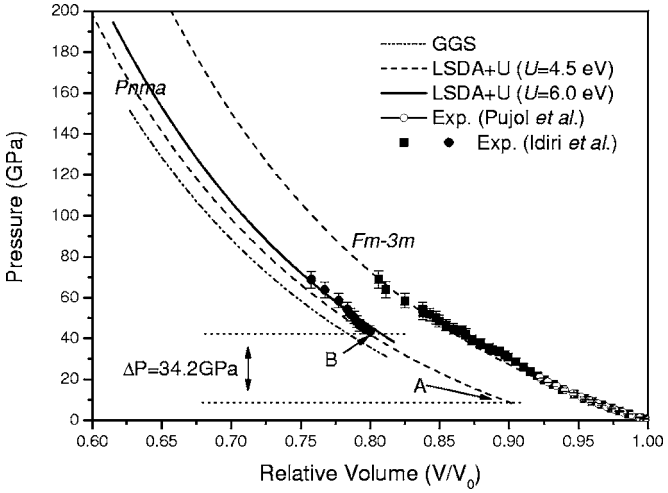

FIG. 3. Calculated compression curves of uranium dioxide along the relative volume compared with experimental measurements. An unexpected large discrepancy of the transition pressure between measurement (point *B*) and theoretical prediction (point *A*) is obtained for the *U*45 case. However, a better result is recovered with $U=6.0$ eV.

coupling decreases the cohesive energy about 0.3 eV for per atom, very close to the energy difference between GGS and LSDA+U at the same volume. Thus, we can expect that neglect of spin-orbit coupling will give an error of 0.012 Å in the lattice constant and 3 GPa in the bulk modulus, the same difference as GGS.

B. Cotunnite phase

To optimize the geometry of the *Pnma* phase at different pressures, the LSDA+U method with $U=4.5$ eV is employed. To avoid the Pulay stress problem (which arises from the fact that the plane-wave basis set is not complete with respect to changes of the volume), structure relaxation calculations are performed at fixed volumes rather than under constant pressures. Then, the pressure is derived from the energy-volume relation. The structure is fully relaxed to optimize all internal coordinates and cell shape, while the symmetry of the *Pnma* space group is kept. The calculated cohesive energy curve is shown in Fig. 2. For comparison the curve of the fluorite phase is also given as a dash-dotted line. It shows that under high pressure the *Pnma* phase becomes stable. A transition pressure of 7.8 GPa is given by the slope of the common tangent as shown in the inset. This value is quite unexpected because it is less than 1/5 of the experiment observation as ~42 GPa.[25] It is very small even if compared with another early measurement that predicted a pressure-induced phase transition to orthorhombic *Cmcm* phase at ~29 GPa (Ref. 40) (which has not yet been repeated by other authors). Nevertheless, the calculated volume reduction of 6.4% agrees well with the observed 7% at the beginning of the cotunnite phase.[25]

Then one may ask what is the matter with it? Is the LSDA+U approximation wrong? From Table I and the comparison of its results at equilibrium volume with experimental data for fluorite phase, we do not think so. Actually, as Fig. 3 shows, LSDA+U gives a compression curve that agrees very well with experiments[25,41] for the $Fm\bar{3}m$ phase, which means that the Hubbard *U* parameter is reasonable and insensitive to pressure. Clearly, we cannot attribute this deviation to the failure of density functional theory or LSDA+U approximation. Figure 3 also shows the *P-V* curve calculated with the GGS approximation. It is worse than LSDA+U, and the transition pressure is also as low as 32 GPa. A hysteresis pressure of about 34 GPa is estimated by using the transition pressures observed in experiment and calculated with $U=4.5$ eV, which are marked by arrows *B* and *A* in Fig. 3, respectively. As discussed in the previous section, this hysteresis of transition pressure would imply that an energy barrier exists. In fact, it is very common for ionic crystal and semiconductors:[33–35] for example, a phase transition of GaN from wurtzite to rocksalt phase, where a large hysteresis of pressure is observed. By using Eq. (4), the cohesive energy curves of the *Pnma* and $Fm\bar{3}m$ phases [Eq. (2) and parameters listed in Table I], and the experimental transition pressure of 42 GPa,[25] we estimate an energy barrier as ~2.1 eV per cell (U_4O_8). This value is large enough to survive the *Pnma* phase to ambient conditions. Unfortunately, no experiment shows this event.

Therefore, the only possibility is that the discrepancy in the *Pnma* phase results from the dependence of *U* on structure (or lattice distortions). We obtained a different $U=6.0$ eV by fitting to the measured *P-V* data of the *Pnma* phase. The resulting energy curve and Morse function parameters are given in Fig. 2 and Table I, respectively. We can see that $U=6.0$ eV gives a quite similar energy curve as $U=4.5$ eV, except the wholly uplifting of the curve. Hereafter, all calculations will be performed for $U=6.0$ eV and $U=4.5$ eV separately, so we assign the former case as *U*6 and the latter as *U*45 for briefness. Although the improvement of the *P-V* curve in *U*6 is limited, as Fig. 3 shows, the calculated transition pressure is corrected to

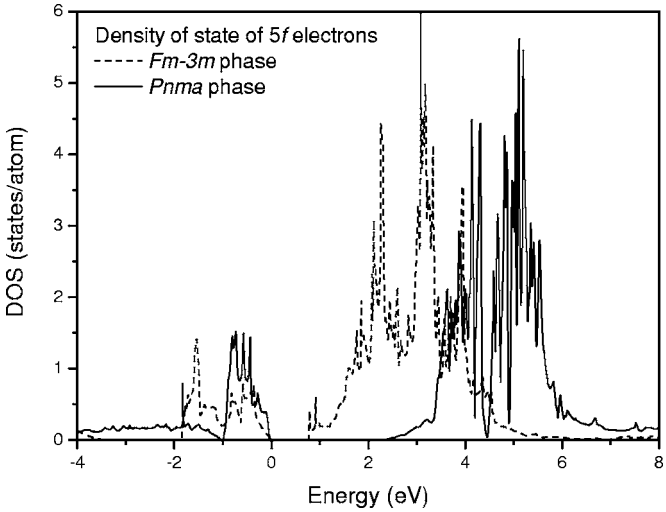

FIG. 4. Electronic density of state for $5f$ states of UO_2 at a cell volume of 131.4 Å^3. The transition to *Pnma* will increase the band gap and shrink the energy region of localized states.

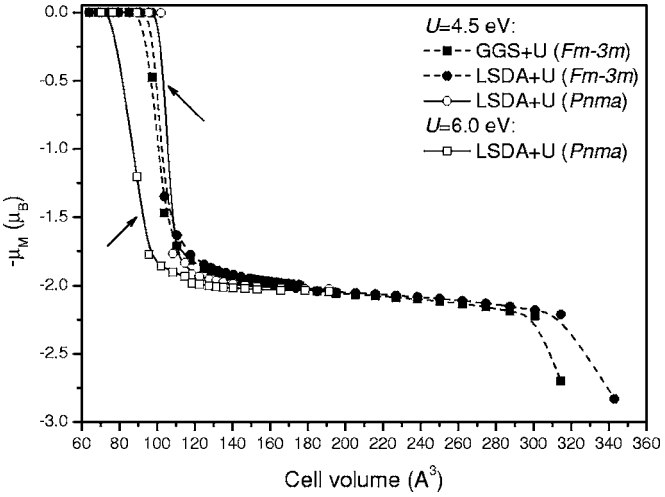

FIG. 5. Variation of the magnetic moment of uranium atoms with cell volume for *Pnma* and $Fm\bar{3}m$ phases. The metallic transition is indicated by the arrows, where a paramagnetic transition also occurs simultaneously.

~38 GPa, almost 5 times the $U45$ case, and in good agreement with the observed 42 GPa. The resulting hysteresis pressure is just 4 GPa, which ends up an energy barrier as 0.018 eV/atom and ignorable at room temperature. Obviously, $U6$ is more credible than $U45$ since it is compatible with the fact that *no Pnma* phase has been observed under ambient conditions. The calculated reduction of volume at the transition from the $Fm\bar{3}m$ to *Pnma* phase is 6.2%, close to the $U45$ case, and also agrees well with experimental data.

Figure 4 compares the DOS of $5f$ states in the $Fm\bar{3}m$ and *Pnma* phases of UO_2 at a cell volume of 131.4 Å^3, close to the transition pressure of the $U6$ case. The most remarkable difference is the increase of the band gap from 0.8 eV in the fluorite phase to 2.4 eV in the *Pnma* phase. As a consequence, unoccupied states also move outwards. Below the Fermi level, different from the fluorite phase where a nearly dispersionless band containing two well-localized $5f$ electrons that lie roughly from −1.8 to 0 eV, in the *Pnma* phase these localized states are further narrowed to start from −1.0 eV, while the valence $5f$ state is expanded from −3.7 to −1.0 eV, too. To completely delocalize the localized $5f$ states, a pressure above 121 GPa is required for $U45$ and beyond 226 GPa for $U6$; we will discuss this in next subsection.

C. High-pressure behavior

The variation of the local magnetic moment of uranium atoms with cell volume is almost the same for *Pnma* and $Fm\bar{3}m$ phases in the $U45$ case, implying that the magnetic property is insensitive to the structural transition in UO_2. As Fig. 5 shows, despite the fact that the GGS+U and LSDA+U approximations give much different cohesive energies for the fluorite phase, the calculated magnetic moment of uranium atoms is very close for a large range of volume, except for the highly expansion region ($V > 300$ Å^3) where atoms trend to be isolated. At equilibrium volume, our calculation gives a moment of $\sim 1.93\mu_B$ in good agreement with previous calculation[21] and slightly larger than observed $1.74\mu_B$.[42] It can be improved by including spin-orbit coupling to $1.88\mu_B$ with an orbit contribution of $0.46\mu_B$. This value is much smaller than all-electron calculations where an orbit moment of $3.6\mu_B$ was predicted.[22]

As shown in Fig. 5, there is a flat level for the local magnetic moment of uranium within moderate pressure range. A transition from antiferromagnetism to paramagnetism is observed at a volume between 102.1 and 108.4 Å^3 for the $U45$ case (equivalent to 121 and 159 GPa in pressure). It corresponds to a volume of 63%–66.4% of the equilibrium volume of the fluorite phase and an effective cubic lattice constant as 86%–88% of the latter phase. Increase U to 6.0 eV postpones the paramagnetic transition to higher pressure as 226–294 GPa, which has an effective cubic lattice constant that is 82%–84% of the fluorite phase at ambient conditions. It is worthwhile to point out that at the same volume a metallic transition also occurs due to complete delocalization of $5f$ states. Figure 6 shows the total DOS of *Pnma* UO_2 under high pressures. We can see that the band gap disappears completely between 226 and 294 GPa. The transition volume is in good agreement with a previous intuitive analysis that a reduction in the effective cubic lattice parameter to 82% of the equilibrium lattice parameter a_0 (of the $Fm\bar{3}m$ phase) is required to have $5f$ states in the conduction band.[43] It is clear that the paramagnetic transition is driven by the delocalization of the two prelocalized $5f$ electrons which become itinerant at this volume, and it is quite reasonable that the metallization is always accompanied by a paramagnetic transition for materials analogous to UO_2 where both band gap and local magnetic moment are attributed to the same localized states.

Below the metallic transition, we also find a new isostructural transition occurring between 80 and 130 GPa for the *Pnma* phase. Figure 7 shows the variation of relative lattice parameters of the *Pnma* phase starting from a respective

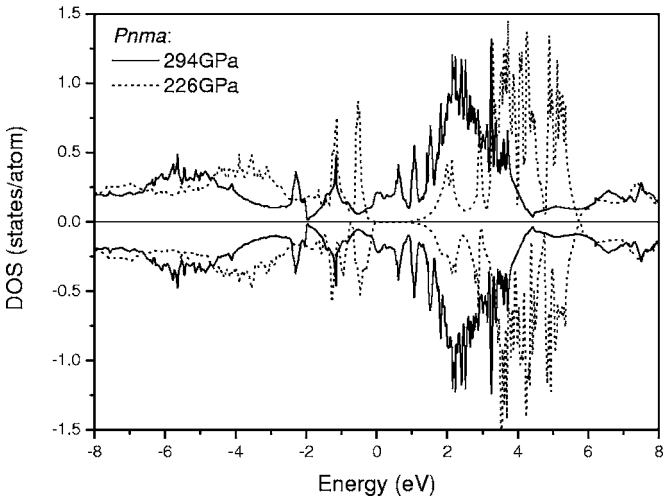

FIG. 6. Total electronic density of states calculated with $U=6.0$ eV for the *Pnma* phase under a pressure of 226 and 294 GPa, respectively. Here the Fermi level is at 0 eV.

transition pressure of the $U45$ and $U6$ cases. Drastic variations were observed for all lattice parameters between 75 and 121 GPa for $U45$ and between 80 and 130 GPa for $U6$, where the smallest axis b has a strong rebound and the middle a is collapsed. At higher pressure, the variations of the relative lattice parameters become smooth and approach isotropic compression. It is a typical structural transition. For the $U45$ case one may wonder whether there is some relevancy between this transition and the metallic one because they adjoin closely in pressure. However, calculation with $U6$ shows that they are irrelevant. By the way, at low pressure the calculated variation of the relative lattice parameters is different from experimental observation, where the smallest axis b is the most compressible whereas the a axis is the most rigid. We do not know the exact reason for this discrepancy at present. But the experimentally observed trend of

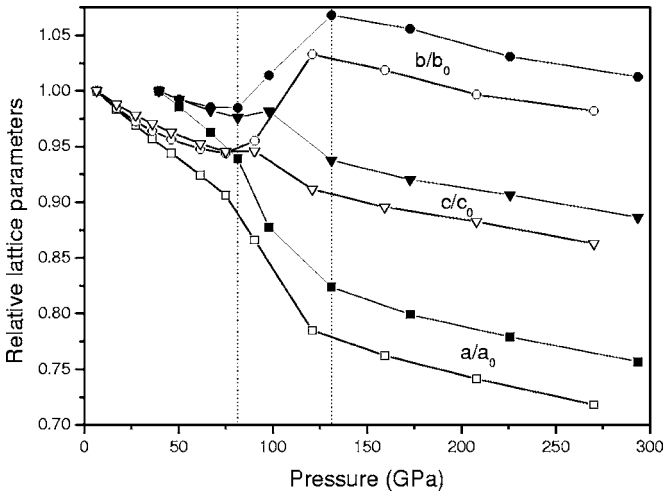

FIG. 7. Pressure behavior of the relative lattice parameters of the *Pnma* phase, where the drastic change in relative lattice constants (region between dotted lines) indicates an isostructural transition. The curves with open symbols are calculated with $U=4.5$ eV, and those solid filled symbols are for $U=6.0$ eV.

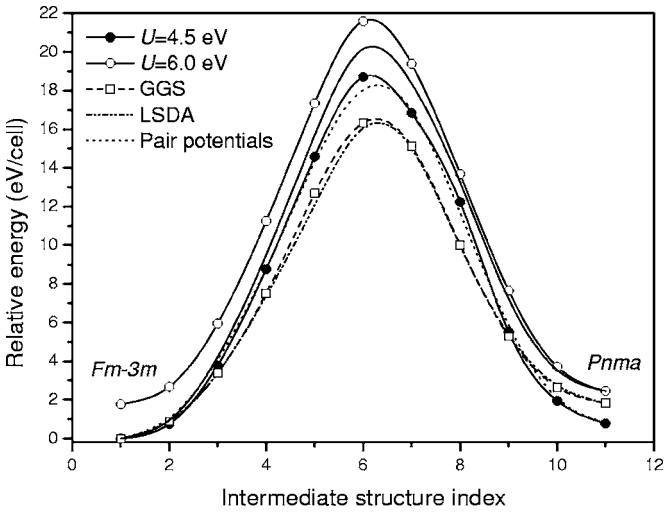

FIG. 8. Relative energies of intermediate structures interpolating the $Fm\bar{3}m$ and *Pnma* phases linearly. The solid line without symbols is obtained with a linear-interpolated value of U between 4.5 and 6.0 eV successively.

relative lattice parameters cannot hold to high pressures because a stronger repulsive force will be present along the shorter axis due to higher compression of electronic states. One can expect a rebound of the smallest axis at higher pressure.

D. Intermediate structures

As discussed in the previous subsections, the value of U depends on structure. This raises a question about the applicability of the LSDA+U method to the intermediate process of structural transitions, since the energy is affected by this term directly. It is impossible to fit the U value for all intermediate structures with experimental data. Therefore, if one attempts to approximately model the transition (or lattice distortions) with just single or several values of U, evaluating the corresponding error becomes important. We do this job for UO_2 by calculating the energy variation along the linear-interpolated intermediate structures between $Fm\bar{3}m$ and *Pnma* phases under ~8 GPa—namely, a candidate transition path for the $U45$ case. In this calculation, no structure optimization is performed.

The result is shown in Fig. 8, where the respective energy of the $Fm\bar{3}m$ phase is set as a reference point for GGS, LSDA, and a classical pair potential model.[11] For LSDA+U, only the energy of the fluorite phase calculated with $U=4.5$ eV is set as reference energy, to take the varying-U effect into account. Since $U6$ fails to model the $Fm\bar{3}m$ phase and $U45$ fails to describe the *Pnma* phase, as the first-level approximation, we interpolate the value of U between these two phases linearly. The result is given in Fig. 8 as the solid curve without symbols. As expected, $U6$ performs well for intermediate structures near the *Pnma* phase while $U45$ becomes better for those close to the fluorite phase. The largest error is 0.15 and 0.14 eV per atom for $U6$ and $U45$, respectively. What is amazing is that the classical

pair potential model outperforms the GGS and LSDA approximations in this test. The former has an error of 0.18 eV per atom and the latter two are 0.32 and 0.34 eV per atom, respectively. It is about 2 times larger than the LSDA+U approximations. This result of the GGS and LSDA approximations is somewhat disappointing. For a unit cell of U_4O_8, it would lead to an error of about 4 eV in cohesive or formation energy. In this sense, the point defect formation energy calculated by Freyss *et al.*[18] is inaccurate and needs further improvement with the LSDA+U method in the uranium defect case due to the large structural distortions. Finally, we would like to point out that the previous conclusion made by Boettger that "the strong correlation effects that are generally believed to produce the observed band gap do not have a significant impact on the binding properties of UO_2"[15] should be treated carefully depending on the structures studied and required precision.

IV. CONCLUSION

The structural behavior of uranium dioxide under pressure up to 300 GPa was investigated by the DFT method with GGS and LSDA approximations plus (or not) Hubbard U correction for strong correlated on-site Coulomb interactions. Comparison with experiment showed that LSDA+U gives the best description for UO_2 in the fluorite phase. However, the calculated transition pressure to the *Pnma* phase with the same U parameter was quite low, indicating that the value of U depends on structure or lattice distortions sensitively. A better value of U for the *Pnma* phase is obtained, which removes the factitious energy barrier predicted by $U=4.5$ eV. The error due to varying of U is estimated as just half of the error given by the GGS and LSDA approximations, showing that LSDA+U is more reliable. Higher pressure leads to an isostructural transition followed by a metallic-paramagnetic transition, which takes place between 226 and 294 GPa with an effective cubic lattice parameter as 82%–84% of the fluorite phase at zero pressure, in good agreement with previous theoretical analysis.

ACKNOWLEDGMENTS

This study was financially supported by the Budget for Nuclear Research of the Ministry of Education, Culture, Sports, Science and Technology of Japan, based on the screening and counseling by the Atomic Energy Commission.

[1] V. Sobolev, J. Nucl. Mater. **344**, 198 (2005).
[2] C. Meis and A. Chartier, J. Nucl. Mater. **341**, 25 (2005).
[3] K. N. Kudin, G. E. Scuseria, and R. L. Martin, Phys. Rev. Lett. **89**, 266402 (2002).
[4] C. J. Pickard, B. Winkler, R. K. Chen, M. C. Payne, M. H. Lee, J. S. Lin, J. A. White, V. Milman, and D. Vanderbilt, Phys. Rev. Lett. **85**, 5122 (2000).
[5] L. V. Matveev and M. S. Veshchunov, JETP **84**, 322 (1997).
[6] L. V. Brutzel, J. M. Delaye, D. Ghaleb, and M. Rarivomanantsoa, Philos. Mag. **83**, 4083 (2003).
[7] Hj. Matzke and M. Kinoshita, J. Nucl. Mater. **247**, 108 (1997).
[8] M. Kinoshita *et al.* (unpublished).
[9] S. Nicoll, H. Matzke, and R. A. Catlow, J. Nucl. Mater. **226**, 51 (1995).
[10] K. Yamada, K. Kurosaki, M. Uno, and S. Yamanaka, J. Alloys Compd. **307**, 10 (2000).
[11] C. B. Basak, A. K. Sengupta, and H. S. Kamath, J. Alloys Compd. **360**, 210 (2003).
[12] J. Hafner, Adv. Mater. (Weinheim, Ger.) **48**, 71 (2000).
[13] V. I. Anisimov, J. Zaanen, and O. K. Andersen, Phys. Rev. B **44**, 943 (1991).
[14] V. I. Anisimov, I. V. Solovyev, M. A. Korotin, M. T. Czyzyk, and G. A. Sawatzky, Phys. Rev. B **48**, 16929 (1993).
[15] J. C. Boettger and A. K. Ray, Int. J. Quantum Chem. **80**, 824 (2000).
[16] T. Petit, C. Lemaignan, F. Jollet, B. Bigot, and A. Pasturel, Philos. Mag. B **77**, 779 (1998).
[17] J. P. Crocombette, F. Jollet, L. Thien Nga, and T. Petit, Phys. Rev. B **64**, 104107 (2001).
[18] M. Freyss, T. Petit, and J. P. Crocombette, J. Nucl. Mater. **347**, 44 (2005).
[19] T. Petit, B. Morel, C. Lemaignan, A. Pasturel, and B. Bigot, Philos. Mag. B **73**, 893 (1996).
[20] S. L. Dudarev, D. N. Manh, and A. P. Sutton, Philos. Mag. B **75**, 613 (1997).
[21] S. L. Dudarev, G. A. Botton, S. Y. Savrasov, Z. Szotek, W. M. Temmerman, and A. P. Sutton, Phys. Status Solidi A **166**, 429 (1998).
[22] S. L. Dudarev, M. R. Castell, G. A. Botton, S. Y. Savrasov, C. Muggelberg, G. A. D. Briggs, A. P. Sutton, and D. T. Goddard, Micron **31**, 363 (2000).
[23] F. Jollet, T. Petit, S. Gota, N. Thromat, M. G. Soyer, and A. Pasturel, J. Phys.: Condens. Matter **9**, 9393 (1997).
[24] R. Laskowski, G. K. H. Madsen, P. Blaha, and K. Schwarz, Phys. Rev. B **69**, 140408(R) (2004).
[25] M. Idiri, T. Le Bihan, S. Heathman, and J. Rebizant, Phys. Rev. B **70**, 014113 (2004).
[26] G. Kresse and J. Furthmüller, computer code VASP, Vienna, 2005.
[27] G. Kresse and J. Furthmüller, Phys. Rev. B **54**, 11169 (1996).
[28] J. P. Perdew, K. Burke, and M. Ernzerhof, Phys. Rev. Lett. **77**, 3865 (1996).
[29] J. P. Perdew and A. Zunger, Phys. Rev. B **23**, 5048 (1981).
[30] P. E. Blöchl, Phys. Rev. B **50**, 17953 (1994).
[31] G. Kresse and D. Joubert, Phys. Rev. B **59**, 1758 (1999).
[32] H. J. Monkhorst and J. D. Pack, Phys. Rev. B **13**, 5188 (1976).
[33] M. S. Miao and W. R. L. Lambrecht, Phys. Rev. B **68**, 092103 (2003).
[34] A. Mujica, A. Rubio, A. Munoz, and R. J. Needs, Rev. Mod. Phys. **75**, 863 (2003).
[35] S. Limpijumnong and S. Jungthawan, Phys. Rev. B **70**, 054104 (2004).
[36] I. J. Fritz, J. Appl. Phys. **47**, 4353 (1976).

[37] This is partially due to the fact that total energy is an integral of the DOS and insensitive to its detailed profile structure. A quite similar situation holds for cluster expansion of the DOS, where the convergence of the DOS is not so good, but the resulting energy and electronic entropy have a good convergence with respect to cluster size. See, for example, H. Y. Geng, M. H. F. Sluiter, and N. X. Chen, J. Chem. Phys. **122**, 214706 (2005).

[38] Y. Baer and J. Schoenes, Solid State Commun. **33**, 885 (1980).

[39] From a point of view based on calculations in this paper and Ref. 22, the criticism of (Ref. 15) about the LSDA+U method on this point is not pertinent.

[40] U. Benedict, G. D. Andreetti, J. M. Fournier, and A. Waintal, J. Phys. (France) Lett. **43**, L171 (1982).

[41] M. C. Pujol, M. Idiri, L. Havela, S. Heathman, and J. Spino, J. Nucl. Mater. **324**, 189 (2004).

[42] J. Faber, Jr. and G. H. Lander, Phys. Rev. B **14**, 1151 (1976).

[43] P. J. Kelly and M. S. S. Brooks, J. Chem. Soc., Faraday Trans. 2 **83**, 1189 (1987).